

# GEMS-Aerosol at ECMWF

**J.-J. Morcrette, A. Benedetti, O. Boucher\*, P. Bechtold, A. Beljaars, M. Rodwell,  
S. Serrar, M. Suttie, A. Tompkins, and A. Untch**

*ECMWF, Shinfield Park, Reading  
RG2 9AX, United Kingdom*

*\*Met.Office, Fitzroy Road, Exeter  
EX1 3PB, United Kingdom*

*Jean-Jacques.Morcrette@ecmwf.int*

## ABSTRACT

Past results on sensitivity of the ECMWF model to different climatological descriptions of aerosols are briefly reviewed. An outline of the plans for GEMS-Aerosol is also briefly given. Preliminary results from the initial implementation of prognostic aerosols in the ECMWF IFS are presented.

## 1. Introduction

Since 1984, the ECMWF forecast model then the Integrated Forecast System (IFS) has only considered climatological aerosols for their direct effect in modulating the radiation fluxes. In October 2003, the representation of tropospheric aerosols was revised and this brought a number of improvements to the model, discussed in Section 2.

As part of the GEMS project (Global Environmental Monitoring System), the ECMWF IFS is being upgraded to include, in its assimilation phase, observational data related to the presence of aerosols (first aerosol optical depth derived from satellite observations in channels sensitive to the presence of aerosols, then satellite radiances in the same channels). A prerequisite for this assimilation of aerosol-sensitive observations is a representation of aerosol processes in the forecast model providing the trajectory. Section 3 outlines the plan for the assimilation, whereas Section 4 describes how the aerosol processes are being introduced into the IFS and Section 5 presents early results obtained when including this first stage of the representation of the aerosol processes in the dynamics and physical processes of the forecast model.

## 2. A change in aerosol climatology

In 1984, maritime, continental, desert, urban, and tropospheric and stratospheric background aerosols were introduced as mean annual quantities by Tanre et al. (1984). For these climatological aerosols, three vertical distributions were considered: the stratospheric background aerosol is homogeneous distributed as a function of pressure above the tropopause, whereas all tropospheric aerosols (except urban-type) have a 3 km (1 km for urban) scale height (Fig. 1).

These aerosols were spatially distributed through a T10 spectral distribution. As seen in Fig. 2, each aerosol type had a very broad spatial pattern fixed over the year.

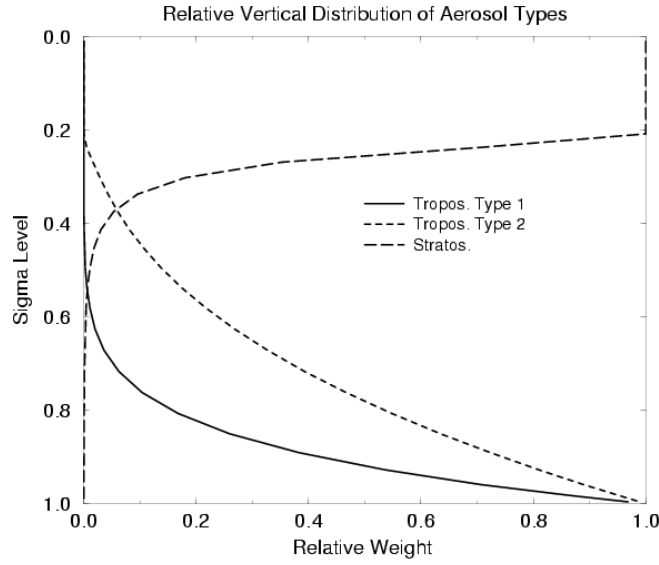


Figure 1: The vertical distribution of the climatological aerosols in the ECMWF model.

In 2002, the representation of tropospheric aerosols was revised: Sea salt, organic and sulfate, desert dust, black carbon replaced the previous aerosol types, with the longwave and shortwave optical properties derived from the GADS model of Hess and Koepke (1997) and the horizontal distributions derived from the monthly mean climatology of Tegen et al. (1997).

In both cases, the aerosols are only used for their impact on the radiation fields, contributing to increasing the optical thickness in both clear and cloudy skies, but without any impact on the condensation of water leading to cloud or precipitation formation.

The change of aerosol climatology, particularly through the reduction of the optical thickness of the desert dust aerosols (a factor two, and appearing only for a few months in NH spring) had a marked impact on the IFS. Tompkins et al. (2005) show an improved analysis of the African Easterly Jet during the JET2000 campaign, together with a better 5-day forecast of the 700 hPa wind (Fig. 3). Rodwell (2005) shows improvements in tropical precipitation, global wind at 925 hPa and geopotential at 500 hPa (Fig. 4).

### 3. Plan for the assimilation of aerosol-sensitive observations

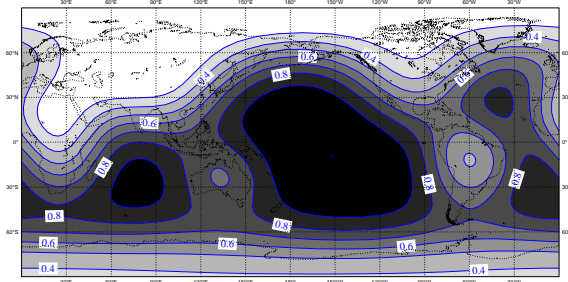
The analysis of aerosol-sensitive observational data will follow the incremental 4-dimensional approach used at ECMWF for other parameters. A description of this approach is given in Rabier et al. (2000), Mahfouf et al. (2000), and Klinker et al. (2000). In the first stage of the project, the analysed aerosols will be considered as passive tracers with no interaction with the radiation or the cloud condensation processes.

The objective is to find  $\mathbf{x}_0$  minimizing the incremental 4-D cost function  $J$

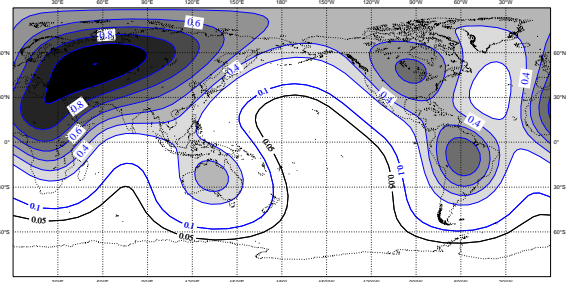
$$J(\delta\mathbf{x}_0) = \frac{1}{2}\delta\mathbf{x}_0^T \mathbf{B}_0^{-1} \delta\mathbf{x}_0 + \frac{1}{2}\sum_i [\mathbf{H}_i \delta\mathbf{x}(t_i) - \mathbf{d}_i]^T \mathbf{R}_i^{-1} [\mathbf{H}_i \delta\mathbf{x}(t_i) - \mathbf{d}_i] \quad (1)$$

where  $\mathbf{B}$  is the background error covariance matrix,  $\delta\mathbf{x}_0 = \mathbf{x}_0 - \mathbf{x}^b$  represents the state vector increments,

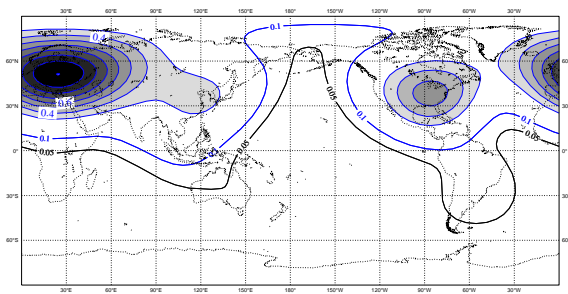
Climatological Aerosols in the ECMWF Forecast System  
Relative Weight  
Maritime Taumax= 0.05 (a)



Climatological Aerosols in the ECMWF Forecast System  
Relative Weight  
Continental Taumax= 0.20 (b)



Climatological Aerosols in the ECMWF Forecast System  
Relative Weight  
Urban Taumax= 0.10 (c)



Climatological Aerosols in the ECMWF Forecast System  
Relative Weight  
Desert Taumax= 0.72 (d)

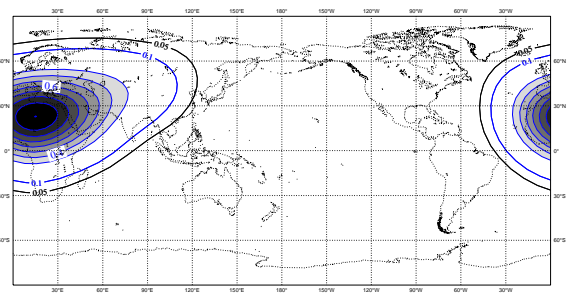


Figure 2: The horizontal weight for the total optical thickness by maritime (a), continental (b), urban (c) and desert aerosols (d). The local optical thickness (N.D.) is obtained by multiplying the weight by 0.05, 0.2, 0.1, 0.72 respectively.

$\mathbf{R}$  is the observation error covariance matrix,  $\mathbf{H}_i$  the linear approximation of the observation operator  $H_i$ ,  $\mathbf{d}_i = \mathbf{y}_i^0 - H_i[M_i(\mathbf{x}^b)]$  is the departure from observation (or innovation vector). In the above,  $\mathbf{x}^b$  is the background model vector, and  $M$  is the model operator.

With such a system, the 4D analysis will work on all variables ( $T, q, wind, O_3$ ) plus  $q_{aer}$ . In contrast to other analysis systems assimilating aerosol information (Collins et al., 2001; Rasch et al., 2001; Weaver et al., 2005) independently of observations relevant to other atmospheric variables, the GEMS-Aerosol system will attempt a consistent and simultaneous analysis of all parameters. For the aerosol observations, we will first consider the optical thickness  $\tau_{aer}^{tot}$  derived, for example, from MODIS (Remer et al., 2005) and in this case  $H$  will be the operator transforming the model aerosol concentrations  $q_{aer}^j$  ( $kg\,kg^{-1}$ ) into the equivalent of the retrieved  $\tau_{aer}$ . Later in the GEMS-Aerosol project, observations of (shortwave) radiances sensitive to aerosols will be considered and  $H$  will likely be an upgraded version of the 6S radiation transfer code (Verrotte et al., 1997) able to simulate radiances in an aerosol-laden clear-sky atmosphere. This will also require a good simulation and/or analysis of the surface radiative properties.

A number of satellite observations, likely to be used, within the development of GEMS-Aerosol, to analyse the atmospheric aerosols, both tropospheric and stratospheric, are presented, with the relevant physical parameters and wavelength of observations in Table 1. Whereas at the development stage, any satellite data could be used, at the end of the GEMS project, only data from operational or long-term satellites will be considered in the IFS.

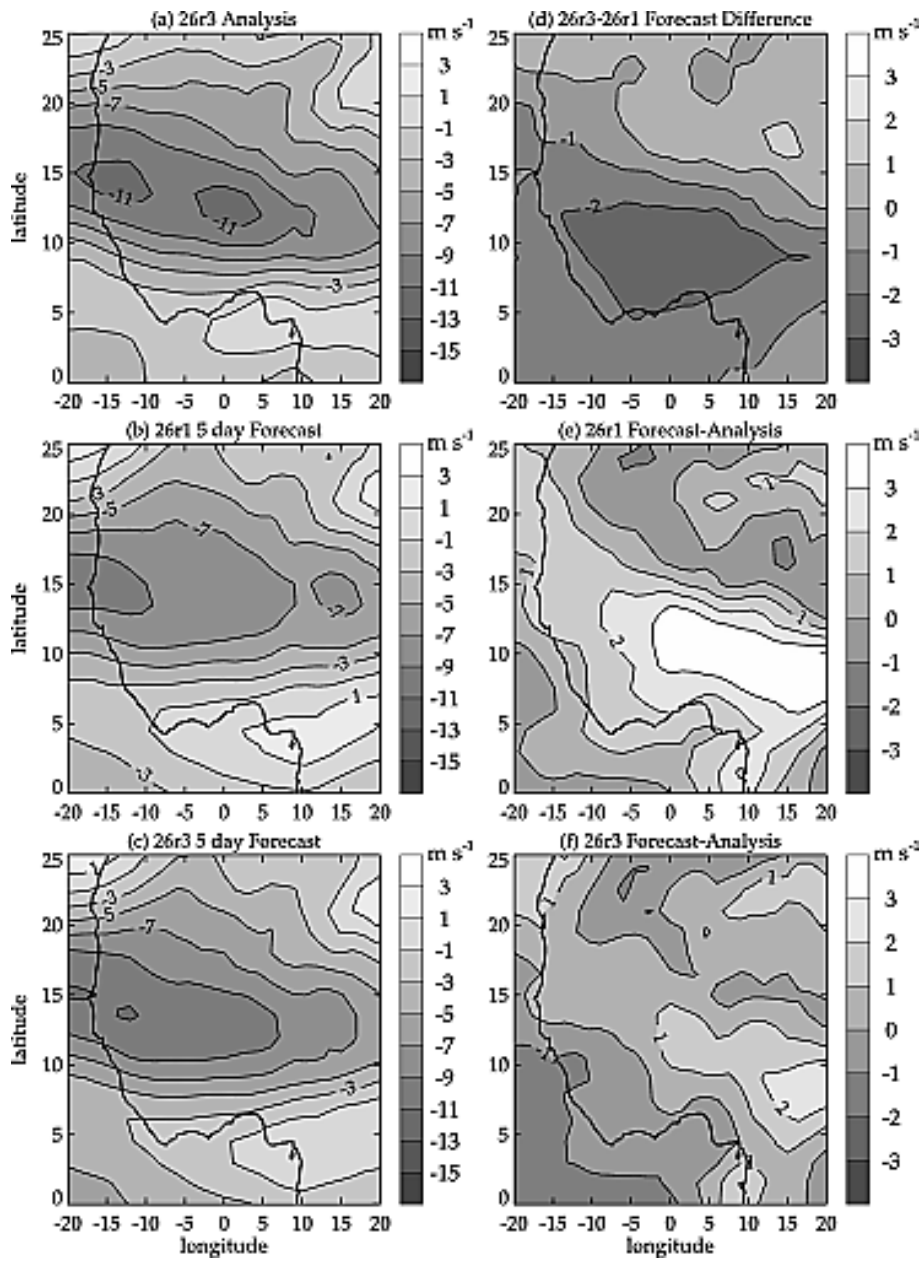


Figure 3: Mean 700 hPa zonal wind from 4 months (June-September 2003) of (a) Daily 12Z Analyses (b) 5-day 26r1 forecast (FC) using old aerosol climatology and (c) 5-day 26r3 FCs using new climatology, (d) FC difference; panel c - panel b, (e) 26r1 FC error; panel b - panel a, (f) 26r3 FC error; panel c - panel a.

$\lambda$ (nm)	Observation type	Instrument
385	extinction	SAGE 3
443	optical depth	MISR
449	extinction	SAGE 3
470	optical depth, reflectance	MODIS (land/ocean)
521	extinction, stratospheric optical depth	SAGE 3
550	optical depth, reflectance*	MODIS (ocean), MISR
602	extinction	SAGE 3
660	optical depth, reflectance	MODIS (land/ocean)
670	optical depth	MISR
676	extinction	SAGE 3
756	extinction	SAGE 3
870	extinction, optical depth, reflectance*	MODIS (land/ocean), SAGE 3 <sup>+</sup> , MISR <sup>**</sup>
1020	extinction	SAGE 3
1240	optical depth, reflectance	MODIS (ocean)
1550	extinction	SAGE 3
1630	optical depth, reflectance	MODIS (ocean)
2130	optical depth, reflectance	MODIS (land/ocean)
3750	optical depth, reflectance	MODIS (land)

\* MODIS only, + exact SAGE 3 wavelength is 868 nm, \*\* exact MISR wavelength is 865 nm.

Table 1: Satellite observations of potential use for GEMS-Aerosol

## 4. Model

In the following, all mentions of the ECMWF model refer to the cycle 29R2 version of the library, set up for a  $T_L$  159 horizontal resolution and 60 vertical levels. Within the model dynamics, the so-called GFL fields allow the advection of tracers to be properly handled in a way consistent with the rest of the dynamics.

For the results presented in this report, the model was run, including parametrisations for the physical processes affecting aerosols (source, dry deposition, sedimentation, wet deposition by large-scale and convective precipitation) from the 1 December 2002 00 UTC to 31 July 2003 24 UTC in a series of 12-hour forecasts starting every 12 hours from the ECMWF operational analyses. The aerosols were started from zero on 1 December 2002 at 00UTC, created from surface emission fluxes, and were free wheeling after that (i.e., the aerosols at the end of a given 12-hour forecast are passed as initial conditions at the start of the next 12-hour forecast). This is in essence not very different from what is done within a transport model, except for the fact that dynamics and all other physical parametrisations are consistent with the aerosol processes. At this stage, there is NO assimilation of any data related to aerosol. Over the past 15 years, a number of transport and climate models have included a representation of aerosol processes and an abundant literature exists on most details of their parametrisation (see Textor et al., 2005 for an overview and an up-to-date list of references). Here, we only reference the main approaches for these various parametrisations and only detail these being introduced in the ECMWF model.

A bin representation is used in this study to include prognostic aerosols of various origins. From the start of the GEMS-Aerosols project, it has been decided to allow the maximum flexibility regarding the limits of the bins for the various aerosols. In the following, the sea-salt aerosols are tentatively represented by 3 bins, with limits at 0.03, 0.5, 5 and 20 microns. Similarly, the desert dust aerosols are represented by 3 bins with limits at 0.03, 0.55, 0.9, and 20 microns. The above limits are chosen so that roughly 10, 20 and 70 percent of the

## Development of a prognostic aerosol package for the ECMWF model

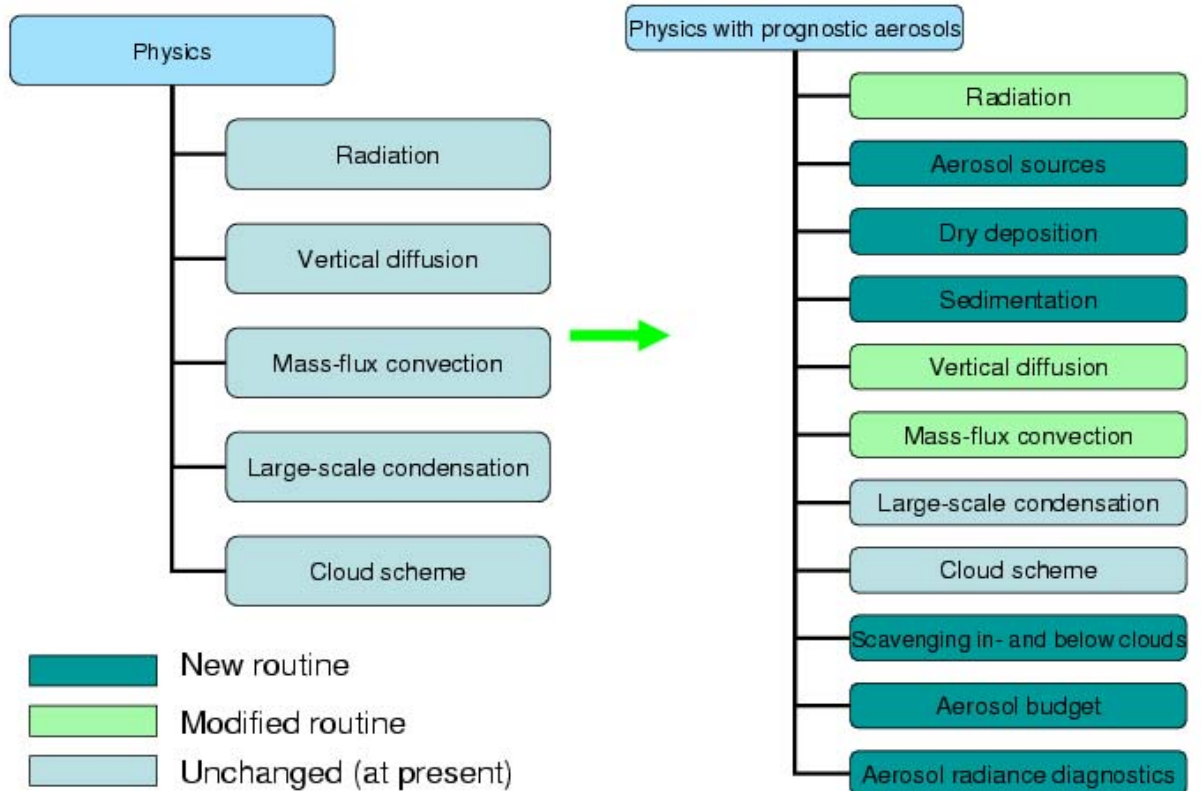


Figure 4: Comparison of calling sequence for the physics without and with routines for prognostic aerosols. Left column: without. Right column: with.

total mass of each aerosol type are in the various bins. A prognostic representation of the tropospheric aerosols related to organic matter, sulfates and black carbon and of the stratospheric aerosols will be considered in a later stage of the GEMS-Aerosol project.

The initial package of ECMWF physical parametrisations dedicated to aerosol processes mainly follows the aerosol treatment in the LOA/LMDZ model (Boucher et al., 2002, Reddy et al., 2005). It includes the sources for sea salt, desert dust, a representation of the sedimentation of all particles, and the wet and dry deposition processes. Recent developments in the ECMWF physical package now allow the vertical diffusion and the mass-flux convection schemes to account explicitly for tracers, thus with aerosols. The wet and dry deposition schemes were directly adapted from the LMDZ model, whereas the sedimentation of aerosols follows closely what has recently been done for ice particles by Tompkins (2005).

#### a. Sources.

Different approaches to sea salt production are reviewed in Guelle et al. (2001) and a detailed description of the processes involved is given in Grini et al. (2002). "Sea spray is generated by wind stress on the ocean surface. Air bubbles, which constitute the whitecaps resulting from breaking waves, burst at the water surface and produce small droplets by means of two mechanisms. Film drops are produced when the thin liquid film that separates the air within a bubble from the atmosphere ruptures. The remaining surface energy of the bubble, after bursting, results in a liquid jet that becomes unstable and breaks into a number of jet drops (Smith et al., 1993). The formation of film and jet drops can be called indirect mechanism. At wind speeds greater than 10-12  $m^{-1}$ , spume drops torn directly from the wave crests by strong turbulence make an increasing contribution to the sea salt and dominate the concentration at larger particle sizes. The formation of spume drops is called the direct mechanism."

The vertical flux of sea salt aerosols is parametrised from the 10-meter wind at the free ocean surface following Monahan et al. (1986)

$$\frac{dF_0}{dr} = 1.373u_{10}^{3.41} r^{-3} (1 + 0.057r^{1.05}) \times 10^{1.19e^{-B^2}} \quad (2)$$

where  $B = (0.380 - \log r)/0.650$ ,  $r$  is the particle radius (in  $\mu m$ ) and  $u_{10}$  the 10-m wind speed (in  $ms^{-2}$ ). The emission flux (in  $m^{-2}s^{-1}$ ) for a size bin ( $i$ ) is obtained by integrating (2) over the size range ( $r_{i1}$  to  $r_{i2}$ ) in the bin to yield

$$F_i(u_{10}) = a_i u_{10}^{3.41} \quad (3)$$

where

$$a_i = \int_{r_{i1}}^{r_{i2}} 1.373r^{-3} (1 + 0.057r^{1.05}) \times 10^{1.19e^{-B^2}} dr \quad (4)$$

A density of  $2160 kgm^{-3}$  is assumed for dry particles. Sea salt production is calculated assuming a 80 percent relative humidity. At this relative humidity, the particle radius will be twice the dry radius (Fitzgerald, 1975), and the density used in the production is thus  $1182 kgm^{-3}$ . The number of particles produced is converted to mass according to

$$M = \frac{4\pi N \rho_p r^3}{3} \quad (5)$$

where  $M$  is the total mass produced in a model grid cell ( $kg$ ),  $N$  is the total number produced,  $\rho_p$  is the particle density, and  $r$  is the radius.

Only the dry mass is added to the bin and transported. Thus no water is transported via the aerosols. Mass is not transferred between bins because of growth. However, wet density and radius are considered for all the size bins when dealing with dry deposition/sedimentation (and radiation processes in the future).

Dust mobilization is sensitive to a wide range of factors including soil composition, soil moisture, surface conditions and wind velocity. Dust uplifting into the atmosphere is mainly initiated by saltation bombardment (sand blasting). Various parametrisations have been developed over the years to represent these processes (Gillette et al., 1980; Tegen and Fung, 1994; Ginoux et al., 2001). Marticorena and Bergametti (1995) developed a sophisticated parametrisation of this process, which requires detailed information on soil characteristics, which was not readily available in the model. For the production of desert dust in the ECMWF model, a preliminary formulation of the source was implemented following Ginoux et al. (2001). First, the areas likely to produce dust are diagnosed for snow-free land with at least 10 percent of bare soil, and the soil moisture below from the wilting point. For them, the flux is a function of the surface wind

$$F_i(u_{10}) = \begin{cases} Su_{10}^2(u_{10} - u_t) & \text{if } u_{10} > u_t \\ 0 & \text{otherwise} \end{cases} \quad (6)$$

where  $u_t$  is a lifting threshold speed depending on soil wetness and particle radius and  $S$  is the source function ( $S = 2 \times 10^{-11} kg s^2 m^{-5}$ ). The main difference with a parametrisation following closely Marticorena and Bergametti's approach is that  $S$ , also called dust emission potential, is here independent of the geography, and we rely on the vegetation cover and soil moisture provided by the model to diagnose which areas are likely to produce a flux of dust.

#### *b. Removal processes.*

Two types of removal processes are considered, the dry deposition including the turbulent transfer to the surface and the gravitational settling, and the wet deposition including rainout and washout of aerosol particles in and below the clouds.

*i. Dry deposition.* The turbulent transfer of particles at the surface is represented as a decrease of the emission flux using a deposition velocity  $v_d$ . A review of the knowledge on dry deposition, taking into account the surface type (ocean or land, vegetation type) is given by Wisely and Hicks (2000). In these preliminary results, the dry deposition to the surface is accounted for through a decrease of the aerosol concentration in the lowermost model layer assuming a flux

$$F_{DD} = Cv_d \quad (7)$$

where  $C$  is the concentration in the first layer above the surface (in  $gm^{-3}$ ),  $v_d$  is the dry deposition velocity, simply function of the particle mode radius and surface type. More sophisticated representations would make  $v_d$  depend on the aerodynamic resistance  $r_a$  and the resistance in the quasi-laminar sub-layer  $r_b$ , linking it to either the vegetation or the wave characteristics.

*ii. Sedimentation.* For the larger aerosols, the most efficient removal process is the gravitational settling (sedimentation). The change in concentration follows the approach developed by Tompkins (2005) for the



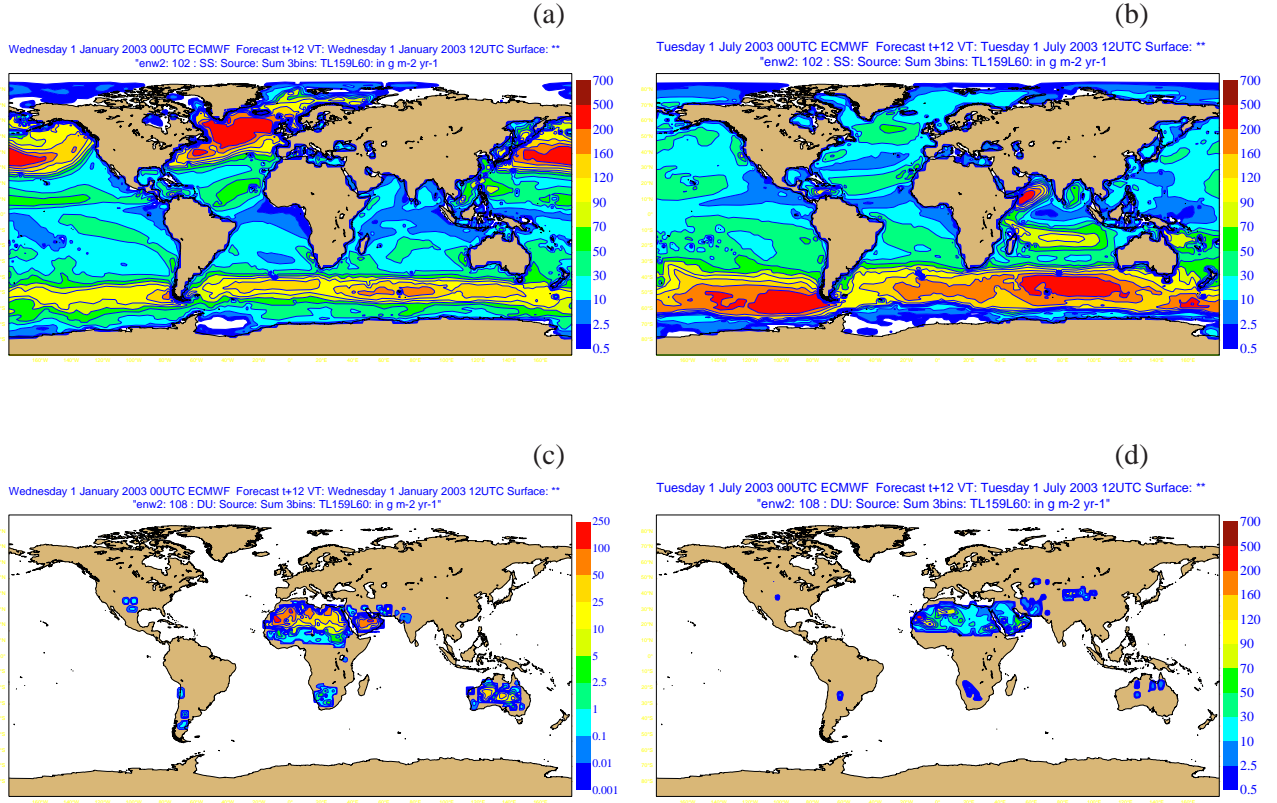


Figure 5: The source of sea salt aerosols (a, b), and dust (c, d) for January (left column) and July 2003 (right column). All quantities are in units of  $\text{gm}^{-2}\text{year}^{-1}$ .

sedimentation of ice. For a concentration  $C$ , including a flux form term for transport at a velocity  $v$ , the change in concentration is given by

$$\frac{dC}{dt} = S + FC + \frac{1}{\rho} \frac{d(\rho v C)}{dz} \quad (8)$$

where the sink term is divided between an explicit slow process  $S$  and an implicit fast process  $F$ . Tompkins (2005) shows that the solution is

$$C_j^{n+1} = \frac{S\Delta t + \frac{\rho_{j-1} v_{j-1} C_{j-1}^{n+1}}{\rho_j \Delta Z} \Delta t + C_j^n}{1 + F\Delta t + \frac{\rho_{j-1} v_j}{\rho_j \Delta Z} \Delta t} \quad (9)$$

The settling velocity  $v_{St}$  for a particle of radius  $r$  is determined by Stokes's law

$$v_{St} = \frac{2\rho_p g}{9\mu} r^2 C_{Cunn} \quad (10)$$

where  $\rho_p$  is the particle density,  $g$  the acceleration of gravity,  $\mu$  is the absolute viscosity of air, and  $C_{Cunn}$  is the Cunningham correction to account for the viscosity dependency on air pressure and temperature.

*iii. Wet deposition.* A review of GCM-type schemes to deal with wet precipitation scavenging can be found in Lee and Feichter (1995) and Rasch et al. (2000). In this study, wet deposition is computed separately for convective and large-scale precipitation using the relevant precipitation flux profiles, and following Giorgi and Chameides (1986) for the in-cloud scavenging.

The scavenging rate ( $s^{-1}$ ) is given by  $W_I = \beta fr$ , with  $r$  the fraction of aerosol included in droplets through dissolution or impaction,  $f$  the cloud volume fraction, and  $\beta$  the rate of conversion of cloud water to rainwater (in  $kgkg^{-1}s^{-1}$ ).  $r$  is set to 0.7 for both sea salt and desert dust. The parameter  $\beta$  at model level  $k$  is computed from the 3D precipitation flux  $P$  (in  $kgm^{-2}s^{-1}$ ) and the model condensed water mixing ratio  $q$  (in  $kgkg^{-1}$ ) as

$$\beta_k = \frac{P_k - P_{k+1}}{\rho_{air,k} \Delta z_k f_k q_k} \quad (11)$$

In these preliminary results, no distinction is made between rain and snow and  $f$  is assumed to represent the full layer.

Below-cloud scavenging is computed considering the volume of space swept by a raindrop during its fallout. The scavenging rate is given by

$$W_B = \frac{3P_r \alpha}{4R_r \rho} \quad (12)$$

where  $R_r$  is an average raindrop radius (set to 1mm),  $\rho$  the water density ( $kgm^{-3}$ ) and  $\alpha$  the efficiency with which aerosols are collected by raindrops. Values of 0.001 and 0.01 for raindrops and snowflakes were selected for  $\alpha$  based on measurements reported in Pruppacher and Klett (1997).

The release at a level  $k$  is equal to the amount scavenged at higher levels multiplied by the fraction of precipitation which is evaporated, with an 0.5 multiplicative factor to account for the fact that raindrops can shrink without evaporating totally. If the incoming precipitation flux totally evaporates in the layer, the aerosols are released totally as well.

### *c. Optical properties.*

Although in this study, the aerosols are not interactive with the radiation scheme, the optical thickness for both sea salt and dust aerosols are evaluated as a diagnostic quantity that could be compared to measurements such as those taken by AERONET (Holben et al., 1998; Dubovik et al., 2002; Kinne et al., 2003). For the 17 shortwave wavelengths (The emission-contaminated  $3.75\mu m$  wavelength is not diagnosed here), the refractive indices were derived from Lacis (2001) for sea salt and interpolated from Dubovik et al. (2002) for desert dust. Then a standard Mie scattering algorithm is applied accounting for the assumed particle size distribution sub-divided in the chosen bins. Optical thickness for sea salt and dust are obtained by summing the individual bin contribution to the optical thickness for each aerosol type.

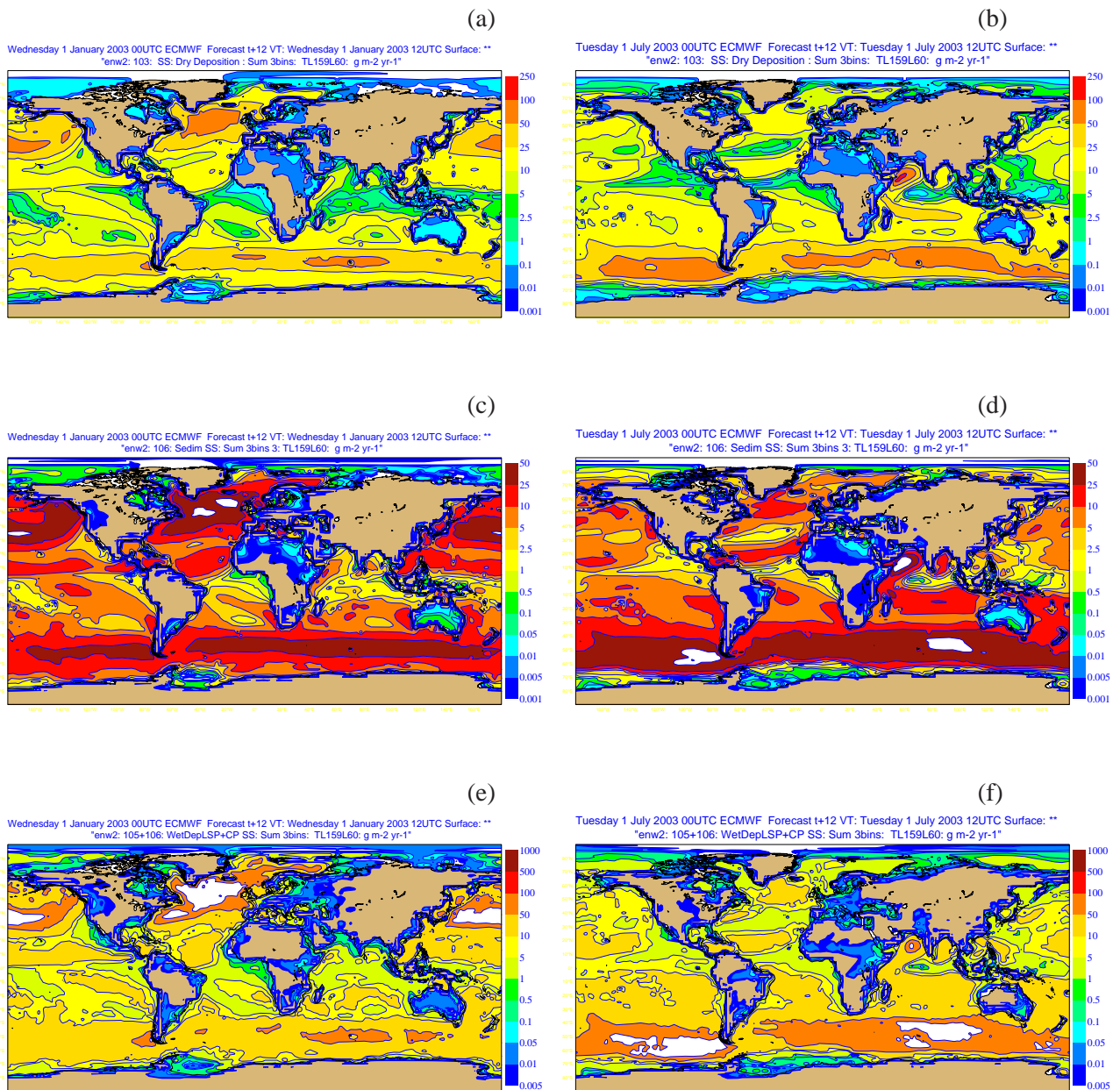


Figure 6: For sea salt aerosols, the dry deposition (a, b), sedimentation (c, d), and wet deposition (e, f) for January (left column) and July 2003 (right column). All quantities are in units of  $\text{g m}^{-2} \text{year}^{-1}$ .

## 5. Preliminary simulations

Starting from null concentrations of aerosols on 1 December 2002 00UTC, the model spins up for about 8-12 days (the time the aerosol content establishes itself), and the results are shown for January and July 2003. Figure 5 presents the sources of sea salt and desert dust aerosols for the months of January and July 2003. The dry deposition, sedimentation, and total wet deposition for sea salt aerosols are shown in Figure 6, whereas

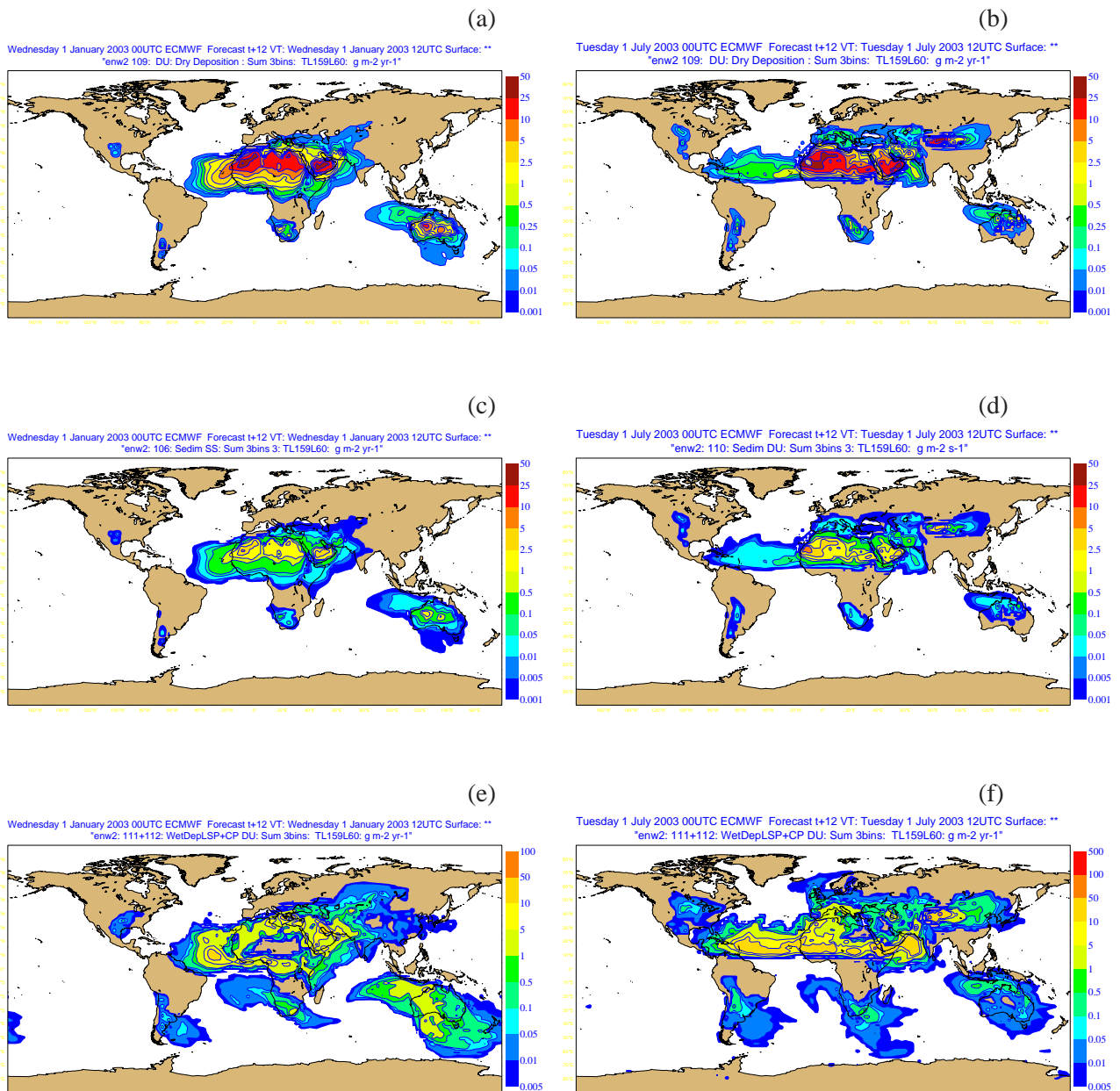


Figure 7: For dust aerosols, the dry deposition (a, b), sedimentation (c, d), and wet deposition (e, f) for January (left column) and July 2003 (right column). All quantities are in units of  $\text{g m}^{-2} \text{year}^{-1}$ .

Figure 7 displays the corresponding fields for the desert dust aerosols. The optical thickness at 550 nm for the two months and the two aerosol types is given in Figure 8. From Figures 5 and 6, it is clear that dry deposition mainly occurs above the source areas, the result of the bigger particles being airborne for a limited period of time. For the smaller particles, a return to the surface is mainly forced by sedimentation and wet deposition. The atmospheric load of aerosols only represent a very small fraction of the aerosols being cycled.

The ECMWF model fields were compared to the equivalent fields compiled within the framework of AERO-

COM ( <http://nansen.ipsl.jussieu.fr/AEROCOM> ), the Global Aerosol Model Intercomparison, for a number of GCMs carrying prognostic aerosols. As discussed by Textor et al. (2005), even for the natural sea salt and desert dust aerosols, there is a wide diversity, not so much in emission, but in the partitioning between wet and dry deposition, and between gravitational settling and turbulent deposition. This results in a reasonable agreement between models as far as total optical thickness is concerned, but different distributions between aerosol types, as well as different vertical distributions of aerosols.

At this preliminary stage, the only message is that the ECMWF model can handle such sea salt and desert dust aerosols reasonably well, and be within the "accepted" diversity of the AEROCOM results.

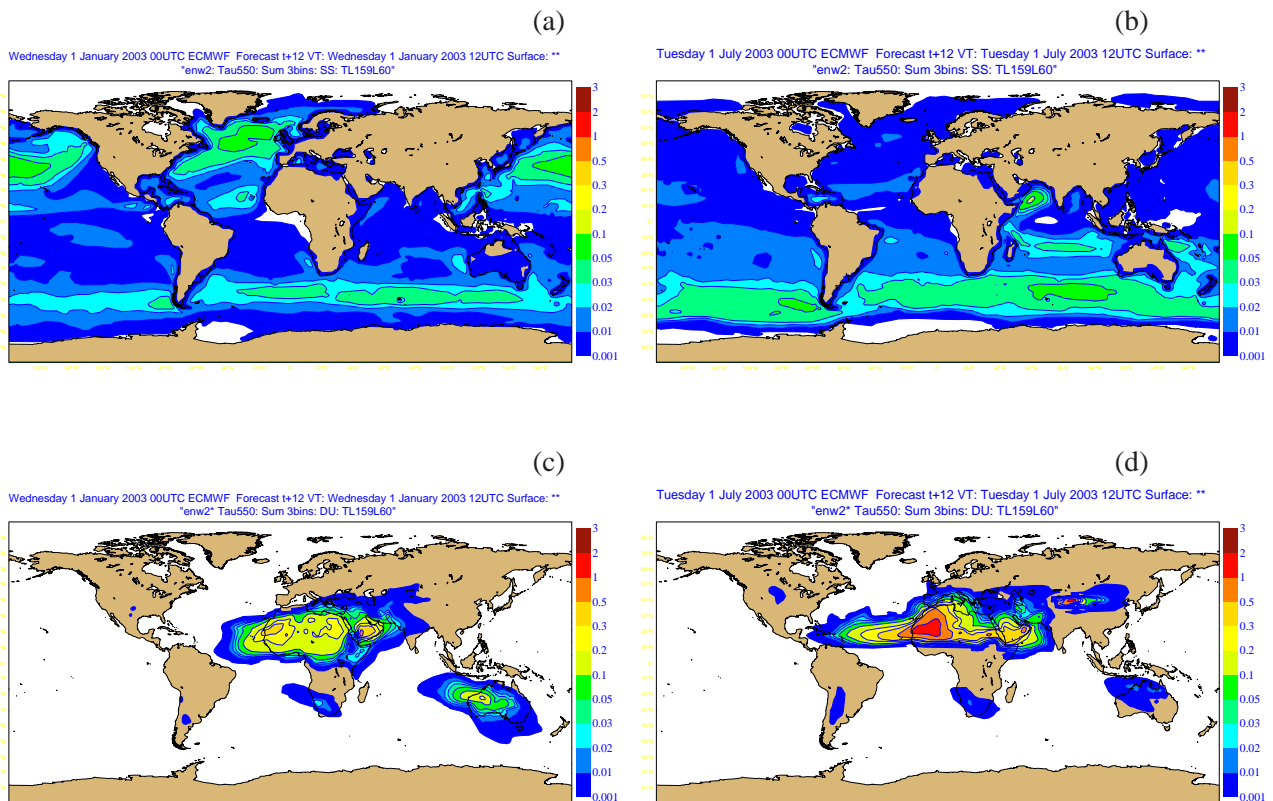


Figure 8: The atmospheric optical depths at 550 nm for sea salt (a, b) and dust aerosols (c, d) for January (left column) and July 2003 (right column).

## Acknowledgements

Thanks to Tony Hollingsworth, the coordinator of the GEMS project, for reviewing this manuscript.

## References

- Boucher, O., M. Pham, and C. Venkataraman, 2002: *Simulation of the atmospheric sulfur cycle in the LMD GCM. Model description, model evaluation, and global and European budgets*. IPSL, Note 23, 26 pp.
- Collins, W. D., P. J. Rasch, B. E. Eaton, B. V. Khattatov, J.-F. Lamarque, C. S. Zender, 2001: Simulating aerosols using a chemical transport model with assimilation of satellite aerosol retrievals: Methodology for INDOEX. *J. Geophys. Res.*, **106D**, 7313-7336, 10.1029/2000JD900507.
- Dubovik, O., B. Holben, T.F. Eck, A. Smirnov, Y.J. Kaufman, M.D. King, D. Tanr, and I. Slutsker, 2002: Variability of Absorption and Optical Properties of Key Aerosol Types Observed in Worldwide Locations *J. Atmos. Sci.*, **59**, 590-608.
- Fitzgerald, J.W., 1975: Approximation formula for the equilibrium size of an aerosol particle as a function of its dry size and composition, and the ambient relative humidity. *J. Appl. Meteorol.*, **14**, 1044-1049.
- Gillette, D.A., J. Adams, A. Endo, and D. Smith, 1980: Threshold velocities for input of soil particles in the air by desert soils. *J. Geophys. Res.*, **85**, 5621-5630.
- Ginoux, P., M. Chin, I. Tegen, J. Prospero, B.N. Holben, O. Dubovik, and S.-J. Lin, 2001: Sources and distributions of dust aerosols simulated with the GOCART model. *J. Geophys. Res.*, **106D**, 20255-20274.
- Giorgi, F., and W.L. Chameides, 1986: Rainout lifetimes of highly soluble aerosols and gases as inferred from simulations with a general circulation model. *J. Geophys. Res.*, **91D**, 14367-14376.
- Grini, A., G. Myrhe, J.K. Sundet, and I.S.A. Isaksen, 2002: Modeling the annual cycle of sea salt in the global 3D model Oslo CTM2: COncentrations, fluxes and radiative impact. *J. Climate*, **15**, 1717-1730.
- Guelle, W., M. Schulz, Y.J. Balkanski, and F. Dentener, 2001: Influence of the source formulation on modeling the atmospheric global distribution of sea salt. *J. Geophys. Res.*, **106D**, 27509-27524.
- Hess, P. Koepke, and I. Schult, 1998: Optical properties of aerosols and clouds: The software package OPAC. *Bull. Amer. Meteor. Soc.*, **79**, 831-844.
- Holben, B.N., T.F. Eck, I. Slutsker, D. Tanre, J.P. Buis, A. Setzer, E. Vermote, J.A. Reagan, Y.J. Kaufman, T. Nakajima, F. Lavenu, I. Jankowiak, A. Smirnov, 1998: An emerging ground-based aerosol climatology: Aerosol optical depth from AERONET. *J. Geophys. Res.*, **106D**, 12067-12097
- Kinne S., et al., 2003: Monthly averages of aerosol properties: A global comparison among models, satellite data, and AERONET ground data, *J. Geophys. Res.*, **108** (D20), 4634, doi:10.1029/2001JD001253.
- Klinker, E. F. Rabier, G. Kelly, and J.-F. Mahfouf, 2000: The ECMWF operational implementation of four dimensional variational assimilation: Part III. Experimental results and diagnostics with operational configuration. *Quart. J. Roy. Meteor. Soc.*, **126**, 1191-1215.
- Lacis, A., 2001: *Refractive Indices of Three Hygroscopic Aerosols and their Dependence on Relative Humidity*, [http://gacp.giss.nasa.gov/data\\_sets/lacis/](http://gacp.giss.nasa.gov/data_sets/lacis/)
- Lee, H.N., and H. Feichter, 1995: An intercomparison of wet precipitation scavenging schemes and the emission rates of  $^{222}\text{Rn}$  for the simulation of global transport and deposition of  $^{210}\text{Pb}$ . *J. Geophys. Res.*, **100D**, 23253-23270.
- Liu, M., and D. L. Westphal, 2001: A study of the sensitivity of simulated mineral dust production to model resolution. *J. Geophys. Res.*, **106D**, 18099-18112.
- Mahfouf, J.-F., and F. Rabier, 2000: The ECMWF operational implementation of four-dimensional variational

- assimilation: II. Experimental results with improved physics. *Quart. J. Roy. Meteor. Soc.*, **126**, 1171-1190.
- Martcorena, B., et G. Bergametti, 1995: Modelling the atmospheric dust cycle. 1: Design of a soil-derived dust emission scheme. *J. Geophys. Res.*, **100D**, 16,415-16,430.
- Monahan, E.C., D.E. Spiel, and K.L. Davidson, 1986: A model of marine aerosol generation via whitecaps and wave disruption, in *Oceanic Whitecaps*, ed. E.C. Monahan and G. Mac Niocaill, eds., D. Reidel, Norwell, Mass., 167-174.
- Pruppacher, H.R., and J.D. Klett, 1997: *Microphysics of Clouds and Precipitation*, 2nd Revised and enlarged edition, Kluwer Academic Publ., Boston, Mass., 954 pp.
- Rabier, F., H. Jarvinen, E. Klinker, J.-F. Mahfouf, and A. Simmons, 2000: The ECMWF operational implementation of four dimensional variational assimilation: Part I: Experimental results with simplified physics. *Quart. J. Roy. Meteor. Soc.*, **126**, 1143-1170.
- Rasch, P.J., J. Feichter, K. Law, N. Mahowald, J. Penner, et al., 2000: An assessment of scavenging and deposition processes in global models: Results from the WCRP Cambridge workshop of 1995. *Tellus*, **52B**, 1025-1056.
- Rasch, P. J., W. D. Collins, B. E. Eaton, 2001: Understanding the Indian Ocean Experiment (INDOEX) aerosol distributions with an aerosol assimilation, *J. Geophys. Res.*, **106D**, 7337-7356, 10.1029/2000JD900508.
- Reddy M. S., O. Boucher, N. Bellouin, M. Schulz, Y. Balkanski, J.-L. Dufresne, M. Pham, 2005: Estimates of global multicomponent aerosol optical depth and direct radiative perturbation in the Laboratoire de Meteorologie Dynamique general circulation model, *J. Geophys. Res.*, **110D**, S16, doi:10.1029/2004JD004757.
- Remer, L.A., Y.J. Kaufman, D. Tanre, S. Mattoo, D.A. Chu, J.V. Martins, R.-R. Li, C. Ichoku, R.C. Levy, R.G. Kleidman, T.F. Eck, E. Vermotte, and B.N. Holben, 2005, The MODIS Aerosol Algorithm, Products and Validation. *J. Atmos. Sci.*, **62**, 947-973.
- Rodwell, M., 2005: The local and global impact of the recent change in model aerosol climatology. *ECMWF Newsletter*, **105**, 17-23.
- Smith, M.H., P.M. Park, and I.E. Consterdine, 1993: Marine aerosol concentration and estimated fluxes over sea. *Quart. J. Roy. Meteor. Soc.*, **119**, 809-824.
- Tanre, D., J.-F. Geleyn, and J.M. Slingo, 1984: First results of the introduction of an advanced aerosol-radiation interaction in the ECMWF low resolution global model, in *Aerosols and their Climatic Effects*, H.E. Gerber and A. Deepak, eds., A. Deepak Publishing, Hampton, Va, USA, 133-177.
- Tegen, I., and I. Fung, 1994: Modeling of mineral dust in the atmosphere: Sources, transport and optical thickness. *J. Geophys. Res.*, **99D**, 22897-22914.
- Tegen, I, P. Hoorig, M. Chin, I. Fung, D. Jacob, and J. Penner, 1997: Contribution of different aerosol species to the global aerosol extinction optical thickness: Estimates from model results. *J. Geophys. Res.*, **102**, 23,895-23,915.
- Textor, C., M. Schulz, S. Guibert, S. Kinne, and the AeroCom participants, 2005: Analysis and quantification of the diversities of aerosol life cycles within AeroCom. *J. Geophys. Res.*, submitted.
- Tompkins, A.M., 2005: *A revised cloud scheme to reduce the sensitivity to vertical resolution*. ECMWF Research Dept Technical Memorandum, 20 pp.
- Tompkins, A.M., C. Cardinali, J.-J. Morcrette, and M. Rodwell, 2005: Influence of aerosol climatology on forecasts of the African Easterly Jet. *Geophys. Res. Letters*, **32**, L10801, doi:10.1029/2004GL022189.

Vermotte, E., D. Tanre, J.L. Deuze, M. Herman, J.-J. Morcrette, 1996: Second Simulation of the Satellite Signal in the Solar Spectrum (6S): An overview. *I.E.E.E. Transaction on Geosc. Remote Sens. TGARS*, **35**, 675-686.

Weaver, C., A. da Silva, M. Chin, P. Ginoux, O. Dubovik, D. Flittner, A. Zia, L. Remer, B. Holben and W. Gregg, 2005: Assimilation of MODIS radiances in a global aerosol transport model. *J. Atmos. Sci.*, submitted.

Wisely, M.L., and B.B. Hicks, 2000: A review of the current status of knowledge on dry deposition. *Atmos. Environ.*, **34**, 2261-2282.